

Curvature-based shape recognition: characterising and analysing voltaje dips

Nitin Sundriyal¹, Juan Ramirez², and Eduardo Bayro-Corrochano¹

¹Centro de Investigación y de Estudios Avanzados del Instituto Politécnico Nacional

²Centre for Research and Advanced Studies Unit Monterrey

August 5, 2023

Abstract

This study employs differential geometric algebra to offer a fresh perspective on voltage sag and swell analysis. By utilising differential geometry, simulated electrical signals can be visualised as curves. This is made possible by describing the instantaneous amplitude of a sinusoidal wave as a curve in Euclidean coordinates. This approach effectively represents the Frenet-Serret frame rotation at each point along the curve. In systems with derivative components, the velocity of the moving frame denotes the rate at which events change, as the Frenet structure is locally defined at every point along the curve. This mathematical representation, utilising the Frenet frame, enhances our understanding of phenomena such as sag and swell, in contrast to traditional approaches that rely on the Clark and Park transformations, which utilise two-dimensional forms to capture the details and portrayal of an occurrence. The work emphasises the depiction of voltage through curves and provides a geometric indicator of the pattern's evolution during operation.

- Article title: **Curvature-based shape recognition: characterising and analysing voltage dips**
- Running head/short title: **characterising and analysing voltage dips**
- Names of all authors in the same order as mentioned in ScholarOne: **Nitin Sundriyal, Juan M. Ramirez, Eduardo Bayro-Corrochano**
- Author's contribution: Nitin Sundriyal: **Investigation, programming, draft.** Juan M. Ramirez: **reviewing, writing, suggestions,** Eduardo Bayro-Corrochano: **reviewing, suggestions..**
- Affiliation of all authors: **Centro de Investigación y de Estudios Avanzados del IPN**
- Postal and Email address of the corresponding author: **Juan M Ramirez. Av del bosque 1145. Zapopan, Jal., 45019, MEXICO. Tel +523337773600. manuel.ramirez@cinvestav.mx**
- Funding information (Please mention "Funding: None" if you have not received any support for your research): **None**
- Conflict of Interest Statement: **The authors of this paper confirm that they do not have conflicts of interest.**
- Permission to reproduce materials from other sources (mention "None" if not applicable for your article): **None**

Curvature-based shape recognition: characterising and analysing voltage dips

Nitin Sundriyal¹, Juan M. Ramirez¹, and Eduardo Bayro-Corrochano¹

¹Centro de Investigación y de Estudios Avanzados del IPN, Unidad Guadalajara-Mexico, 45019

email: nitin.sundriyal [manuel.ramirez][eduardo.bayro]@cinvestav.mx

Abstract This study employs differential geometric algebra to offer a fresh perspective on voltage sag and swell analysis. By utilising differential geometry, simulated electrical signals can be visualised as curves. This is made possible by describing the instantaneous amplitude of a sinusoidal wave as a curve in Euclidean coordinates. This approach effectively represents the Frenet-Serret frame rotation at each point along the curve. In systems with derivative components, the velocity of the moving frame denotes the rate at which events change, as the Frenet structure is locally defined at every point along the curve. This mathematical representation, utilising the Frenet frame, enhances our understanding of phenomena such as sag and swell, in contrast to traditional approaches that rely on the Clark and Park transformations, which utilise two-dimensional forms to capture the details and portrayal of an occurrence. The work emphasises the depiction of voltage through curves and provides a geometric indicator of the pattern's evolution during operation.

Keywords ABC signature, Curvature, Frenet Frame, Power quality, Sag, Swell

1. Introduction

Voltage drops often result from fault currents flowing through the power system's impedance to the fault's origin. As a result, power outages caused by transmission or distribution problems might impact thousands or only a few customers. On the other hand, a problem with a transmission line may harm sensitive equipment hundreds of kilometres away. This paper studies failure simulations in the three-phase system to analyse voltage drops.

In the case of voltage sags, their distinctive non-rectangular shape arises from the increased starting current of motors. Previous works have primarily focused on characterising and identifying sags using the space vector approach [1]-[4]. Intriguingly, a recent study employed a 3-D polarisation ellipse parameter for sag quantification [5]. The Clark transform has been commonly used in earlier works on space vectors, which translates a three-phase signal into contra-rotating phasors and a zero-sequence component. However, considering the transient voltage dips and spikes caused by unforeseen failures, a rotating frame is a more suitable approach for analysing this scenario. While some efforts have been made to address this issue [6, 7], their effectiveness has yet to be questioned [8, 9]. In this study, we propose a characterisation of sags using the Frenet or TNB frame. Notably, variations in the instantaneous voltage values are inherently local, independent of any external reference velocity.

Differential geometry is a branch of mathematics that investigates the geometry of smooth manifolds, also referred to as soft forms and spaces. It encompasses various mathematical concepts, including differential and integral calculus and linear and multilinear algebra. Differential geometry connects with geometric analysis, which involves studying geometrical elements within the theory of differential equations. The TNB frame, for instance, elucidates the directional aspects of particle motion on a space curve, signifying the particle's heading (T), turning (N), and twisting (B). TNB or Frenet-Serret equations are commonly employed to describe particle motion in space. As the behaviour of sinusoids can be viewed as a time-varying phenomenon, the study adopts differential geometry, precisely the Frenet frame, to investigate this domain.

An overview of the IEEE Standard 1159-2019 for power quality monitoring is provided in this section [10]. Although there are several power quality phenomena, like voltage fluctuation, harmonics, flicker, etc., voltage sag and swell are approached in the present work. However, other issues can also be handled with the provided framework. Table I demonstrates the sag characteristic [11], which can be due to the type of fault, transformer connection, or load connections.

1.1 *Contribution and Outline*

The paper's most significant originality is:

New perspective: an innovative geometric analysis method that describes sags and swells as curvature functions is proposed.

Enhanced understanding: using differential geometry and the Frenet frame provides a comprehensive understanding of voltage sags and swells. By representing electrical signals as curves in Euclidean coordinates, the study captures the intricacies of these phenomena visually and intuitively. This curve-based representation enhances comprehension compared to traditional approaches, enabling a deeper insight into their behaviour.

Geometric Indicator: The work introduces a novel geometric indicator accompanying the curve-based representation of voltage sags and swells. This indicator is valuable for analysing the patterns and their evolution during operation. It provides a visual and quantitative means to assess the development of these phenomena, enriching the interpretation of their impact on electrical systems.

Comparative Analysis: A comparative analysis highlights the advantages of the proposed approach over traditional methods like the Clark and Park transformations. The Frenet frame-based analysis surpasses the limitations of two-dimensional forms, offering a more detailed and accurate representation of voltage sags and swells. This comparative analysis underscores the superiority of the proposed methodology in capturing the intricate details of these phenomena.

Table I: sag characteristics

Category	Duration	Voltage magnitude
1. Instantaneous		
1.1 Sag	0.5–30 cycles	0.1–0.9 p.u.
1.2 Swell	0.5–30 cycles	1.1–1.8 p.u.
2. Momentary		
2.1 Interruption	0.5 cycles – 3s	< 0.1 p.u.
2.2 Sag	30 cycles – 3s	0.1–0.9 p.u.
2.3 Swell	30 cycles – 3s	1.1–1.4 p.u.
2.4 Voltage imbalance	30 cycles – 3s	2%–15%
3. Temporary		
3.1 Interruption	>3 s – 1 min	< 0.1 p.u.
3.2 Sag	>3 s – 1 min	0.1–0.9 p.u.
3.3 Swell	>3 s – 1 min	1.1–1.2 p.u.
3.4 Voltage imbalance	>3 s – 1 min	2%–15%

2. Incorporating Geometrical Algebra and Differential Geometry in the Presented Work

The differential geometry of curves is concerned chiefly with the local properties of trajectories or curves. A path an object takes through space is referred to as a curve. By incorporating curvature and torsion in three-dimensional space, the Frenet Serret equations determine the gradient of three orthonormal vector fields forming the Frenet frame, which is vital for studying curves.

This article presents space curves derived from a mechanical system's motion curves, where the following parameters are defined.

Position

Velocity

Acceleration

Jerk

All the above motion parameters can be parameterised in the time (t) or arc length (s). The Jerk vector in motion denotes a moving vector's acceleration change. Here it is mentioned just for informative purposes. In the present work, it is utilised for calculating torsion. Position (1), velocity (2), acceleration (3), and Jerk (4) can be parameterised (in time) (1)-(4), and $e_1, e_2, \text{ and } e_3$, become the Euclidean basis of the system. The following formulations are done using the framework in the 3D geometric algebra in G_3 [12]; x, y, and z represent the position.

$$r(t) = x(t)e_1 + y(t)e_2 + z(t)e_3 \quad (1)$$

$$v(t) = \frac{dr(t)}{dt} = \frac{dx(t)}{dt} e_1 + \frac{dy(t)}{dt} e_2 + \frac{dz(t)}{dt} e_3 \quad (2)$$

$$a(t) = \frac{dv(t)}{dt} = \frac{d^2x(t)}{dt^2} e_1 + \frac{d^2y(t)}{dt^2} e_2 + \frac{d^2z(t)}{dt^2} e_3 \quad (3)$$

$$J(t) = \frac{da(t)}{dt} = \frac{d^3x(t)}{dt^3} e_1 + \frac{d^3y(t)}{dt^3} e_2 + \frac{d^3z(t)}{dt^3} e_3 \quad (4)$$

In differential geometry, the focus is on the osculating bivector, the curve's curvature, and its torsion, in addition to the four parameters listed above (1)-(4). In standard calculus, curvature and torsion are regarded as scalars, but in differential framework, they are treated as bivectors and tri-vectors [13, 14].

Equation (5)-(12) specifies the Tangent (T), Normal (N), and Binormal (B), as well as the curvature and torsion, of a Frenet Serret frame.

A tangential vector (T) is the displacement between two points on a curve: the tangent vector and the velocity vector, v , are in the same direction.

$$T(t) = \frac{v(t)}{|v(t)|} \quad (5)$$

The normal vector is defined as

$$N = \frac{T'}{|T'|} \quad (6)$$

where T' is the derivative of (5)

A binormal is a plane that contains a tangent, and a normal vector is defined as

$$B = T \times N \quad (7)$$

(5)-(7) gives the orthonormal vectors of the Frenet Serret frame. Consequently, the derivative of these vectors can be provided by (8)-(10).

$$\frac{dT}{ds} = \kappa N \quad (8)$$

$$\frac{dN}{ds} = \tau B - \kappa T \quad (9)$$

$$\frac{dB}{ds} = -\tau N \quad (10)$$

where κ and τ are curvature and torsion [13] of the curve and are given mathematically as

$$\kappa(t) = \frac{\|r'(t) \times r''(t)\|}{\|r'(t)\|^3} \quad (11)$$

Curvature is a measure of change in the tangent vector or the bending in the shape of the curve.

$$\tau(t) = \frac{(r'(t) \times r''(t)) \cdot r'''(t)}{\|r'(t) \times r''(t)\|^2} \quad (12)$$

Torsion is the change in the binormal vector or the twisting of the curve.

Geometrically, $\kappa(t)$ is a bivector, and $\tau(t)$ is a tri-vector.

Based on (5)-(12), the *TNB* or Frenet frame can be represented as (13)

$$\begin{pmatrix} T' \\ N' \\ B' \end{pmatrix} = \begin{pmatrix} 0 & \kappa & 0 \\ -\kappa & 0 & \tau \\ 0 & -\tau & 0 \end{pmatrix} \begin{pmatrix} T \\ N \\ B \end{pmatrix} \quad (13)$$

Curvature can be perceived as a curving phenomenon. For instance, a straight line has curvature (κ)=0; however, when this straight line is bent into an elliptical or circular shape, the κ is non-zero. Torsion is the change in the binormal vector. It can be perceived as a twisting of a curve or change in the plane spanned by (7), it also represents the cross product, defined in geometric algebra G_3 , and its result is a vector. In DG, the binormal vector precisely τ detects the change in angle or rotation in degrees. The ratio $-\tau/\kappa$ is a critical aspect, as the elliptical nature is defined for the curve by this ratio. This aspect can be considered as a supplementary concept to the shape index (SI) defined for quantifying voltage sag.

The ratio of curvature and torque give rise to different shape in DG. For example, if it is constant, it forms a helix. The angle of rotation for an elliptical shape can be evaluated as

$$\int_0^L(s) ds = \theta(L) - \theta(0) = 2\pi I \quad (14)$$

where θ is the inclination angle spanned by the curve when it moves between two points (p and q), Fig.1, and I stands for the curves' rotation index. Such an angle can be positive or negative based on the direction of movement.

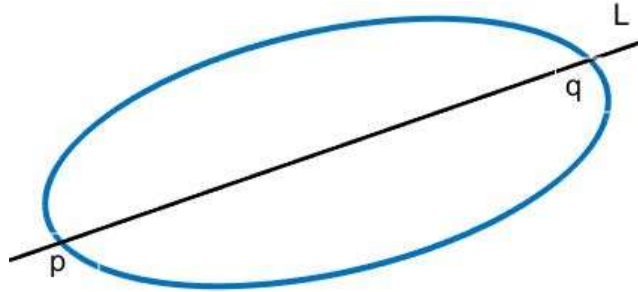


Figure 1. Rotation angle based on κ

The angle between two curves can be evaluated more straightforwardly by taking the scalar or dot product between their respective Tangents in local coordinate or Frenet frame.

Conversely,

$$\cos\theta = \frac{\text{dot}(T, T_s)}{|T||T_s|} \quad (15)$$

T denotes the Tangent vector of a normally operating system, and T_s represents the Tangent vector of a malfunction event. The tilt can be computed using the relation provided in geometrical algebra [14]. However, curvature alone is sufficient to provide information on sag and swell. This data shows how the suggested

method aligns with established practices while shedding new light on voltage dips and spikes. The elliptical aspect of the three-phase analysis is stated in the range of κ from non-negative values to large positive ones. Previous research on sag and swell provides a somewhat convoluted explanation of their elliptical character because they depend on an eclipse's major and minor axis. Furthermore, phasor motion along real and imaginary axes is required for the sag signature, often known as the ABC signature.

3. ABC Signature

The IEC and IEEE standards for describing voltage dips use a single voltage and a single time. This makes the characterisation easier, as well as its interpretation and use in statistical approaches. However, this technique has its downsides; essential data needs to be included when estimating the equipment's performance based on the characteristics of individual dips or the statistics of the dips as a whole. On the other hand, no system can quantitatively compare different sets of features. The three-phase imbalance of the sag and the fact that it is not rectangular will likely present the most difficulties. Examples include voltage dips in many stages and voltage dips that significantly impact motor loads and transformer saturation. In addition, multistage voltage dips can occur because of fault growth because the magnitude of the voltage drops at different times throughout the event. These voltage drops defy categorisation using the stated single-event features [15].

According to the ABC categorisation, there are seven different forms of basic voltage sag. Equation and phasor form representations are shown in Fig. 2, adopted from [14], with phase A as the reference point. E_1 is an indicator of the pre-event voltage in phase a. It brings to mind the equivalence in a balanced system between the voltage in phase a and the voltage in the positive sequence. V is used to signify the voltage that dropped inside the phase or between phases affected by the sag.

Sag and swelling are the most frequent events in a system because of a failure or the abrupt start of large industrial motors. These incidents are more significant since they negatively affect end-user equipment. The Frenet frame, essentially an analytical mathematical method for assessing voltage as a curve, can be utilised for their characterisation based on the local property of curves. First, the voltage wave or curve's orthonormal vectors T , N , and B and the parameters like κ and τ are defined as the rate of change of tangent and change in binormal, respectively.

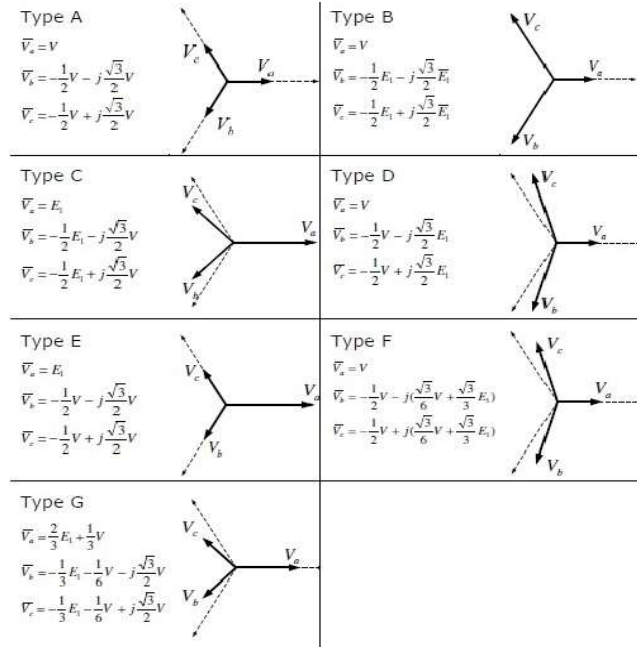


Figure. 2 ABC classification of sag

Curvature (κ), which describes the path that the curve takes through space, is an essential component to consider when imagining voltage in the form of a curve. Because the value of κ changes whenever there is a change in the voltage (for example, a sag or a swell). This value may be used as an index to track the degree to which the voltage has shifted or simply the depth (d) of sag. Although this idea is relatively new in power systems, it has already been used to analyse curves in geodesic control, robotic control, and vehicle trajectory planning. [15,16,17]. F. Milano, through his work on frequency, has recently introduced differential geometry applications [18,19].

A sag signature may be identified by comparing a sagging structure's geometry and inclination angle to a healthy one (without sag). This has been done in previous sag characterisation studies [20,21,22]. The work presented in [20,21,22] talks about the sag characterisation using ellipse major and minor axis and zero sequence components by utilising Clark and Park transform; the same geometrical aspect is shown in this study, in general, the relationship holds the following property.

Curvature and Major Axis: Generally, the curvature tends to be larger near the ends of the major axis of an ellipse. This means that the curve deviates more from being a straight line at these points, resulting in a higher curvature.

Curvature and Minor Axis: The curvature is typically smaller near the points along the minor axis of an ellipse. These points exhibit less deviation from a straight line, resulting in a lower curvature than the ends of the major axis.

Using the orthonormal Tangent vectors or velocity vectors of the system without sag and the simulated sag event, inclination angles may be calculated in the Frenet frame (15). Unlike prior studies that have used phasor representation to evaluate the orientation or tilt angle between the locus of the health system and the sag event

while analysing three-phase voltage sag or swell, the current investigation does not use phasor representation. Summing up the entire process of generating orthonormal vectors in Euclidean space, the algorithm can be summarised in Fig.3.

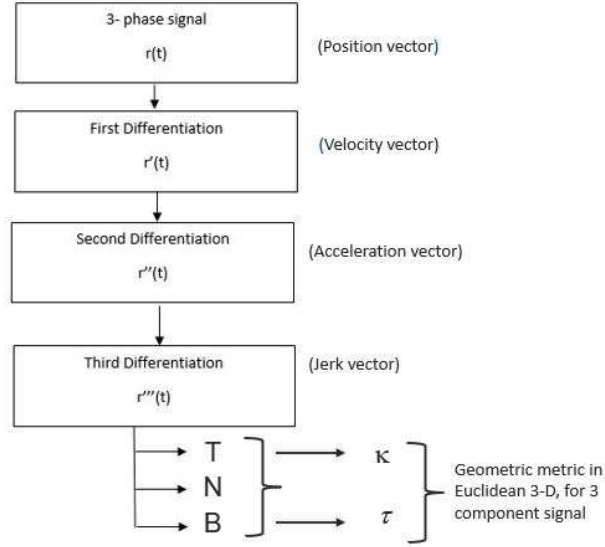


Figure 3. Differential geometry algorithm

where $r(t) = V_a(t)e_1 + V_b(t)e_2 + V_c(t)e_3$ represents the parametric equation of three component voltage signals in time. A detailed analysis of this approach is shown through the presented case studies.

4. Case studies

Four case studies of a three-phase system are presented to demonstrate the above mathematical background, which can be seen as an analogy in practical scenarios. In all the presented cases, the sag or swell event on the phase is compared to the healthy operating system (nominal condition). The p.u. Notation is used for all of the voltages.

Case 1: Sag in single phase (0.1 p.u.)

A line to ground fault (LG) can be attributed to a dip in one phase of a three-phase system, (5)-(7) represents the three individual phases of the simulated system respectively, and $\beta=120^\circ$ is the corresponding angular separation among phases.

$$V_a = V_m \sin(\omega t) \quad (16)$$

$$V_b = V_m \sin(\omega t - \beta) \quad (17)$$

$$V_c = V_m \sin(\omega t + \beta) \quad (18)$$

for sag modelling, the duration is one second

$$vd = 3 < t < 4(\text{time window})$$

and the percentage reduction in voltage during the fault period, also known as depth of sag, is given by

$$d = \frac{vsag}{vm} \quad (19)$$

and sag occurrence in phases a , b , and c is defined by (20)

$$\begin{aligned} V_a(vd) &= V_a(vd)d \\ V_b(vd) &= V_b(vd)d \\ V_c(vd) &= V_c(vd)d \end{aligned} \quad (20)$$

Under normal circumstances, i.e., a system with no variation in voltage, a three-dimensional vector in the time domain may be translated into a single geometric object using the Frenet frame, an ellipse (3 to 1 mapping). Fig. 4. This mapping can be considered a spatial image set as $V(\mathbb{R}) \subset \mathbb{R}^3$. In phase a, a sag of 0.1 p.u. Causes the corresponding curve to alter its trajectory. It is inclined to the elliptical shape representing the healthy system Fig.5(b). The change in curvature value can be detected. It can be reported as a sag event since curvature implies a shift or modification in geometric meaning. Fig. 6. Notice that as the depth of sag increases, κ decreases.

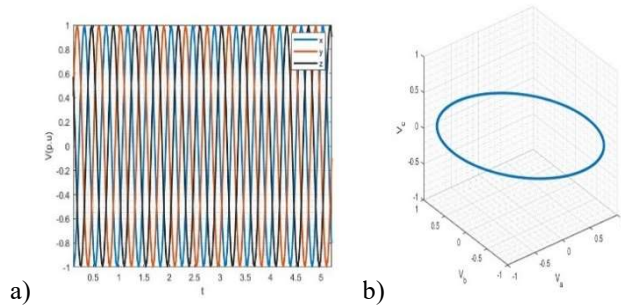


Figure 4 (a) p.u. Voltage Healthy State, (b) Voltage in TNB Frame

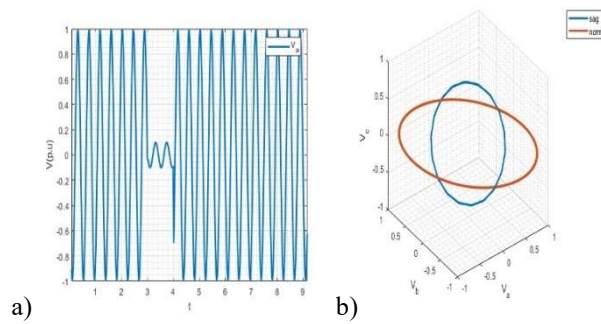


Figure 5 (a) voltage sag in phase a, (b) sag in TNB frame(blue)

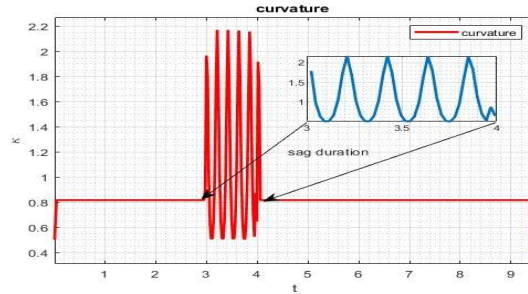


Figure 6. Curvature before, during, and after sag

The sag characterisation in differential geometry can be depicted by a curvature index specifying a range between the maximum and minimum curvature values. These values are chosen because, in between, there are various curvature values defined for different time instants. The curvature at a specific time instant is a scalar value illustrated every moment. From Fig.6, a sag event has an oscillatory nature of curvature values during a sag event, which shows that during a dip or sag, the voltage curve trajectory experiences a sharp change in its steady state. This exciting notion allows us to propose a curvature index for voltage variation. The depth of dip d can be related to the curvature value for defining a relation between d and κ ; other cases are also investigated in the following examples. Typically, when voltage is shown as a curve, the fluctuation in the voltage wave (i.e., sag) is included, and Fig. 7 additionally provides information about the time instant.

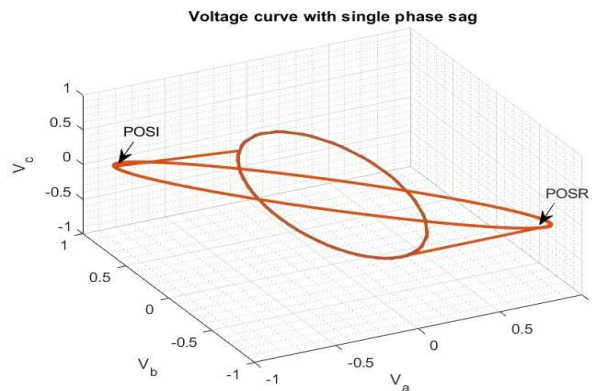


Figure 7 Complete voltage trajectory with sag.

On the curve's trajectory, it is simple to pinpoint the sag initiation (POSI) and retardation (POSR), respectively. But to make things more precise, the sag event and regular behaviour (Balanced scenario) has been handled independently to show the inclination between the two.

Case 2: Sag in single phase (0.9 p.u.)

The same voltage set as for case 1 is adopted for this case. The only difference is $V_{sag} = 0.9$. For a sag of 0.9 p.u., results are presented in Fig. 7(a), and the curvature index is in Fig. 8(b).

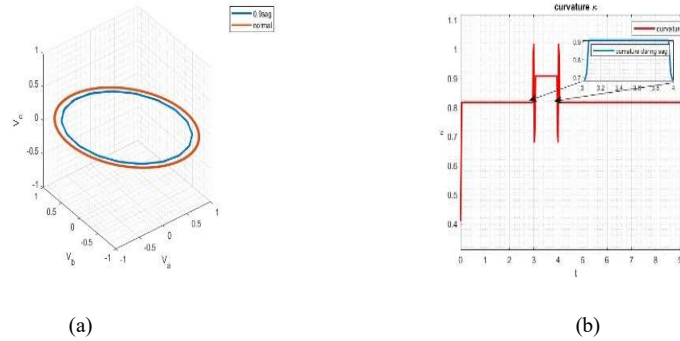


Figure 8 (a) TNB frame(sag 0.9 p.u.) (b) curvature index

If d is the depth of sag, then

$$d \propto \frac{1}{\kappa} \quad (21)$$

Also, the inclination angle during sag is a function of κ , as the curvature is the inverse of the sag depth. The inclination angle is zero for the most severe occurrence, a three-phase sag. The curvature oscillates at a higher value, which may be thought of analytically as the severity measure.

Therefore, empirically the tilt (angle) measure can be approximated by the relation in (22),

$$\kappa \propto \frac{1}{\theta} \quad (22)$$

Thus, the curvature index effectively indicates the voltage variation during a fault or transient condition.

Case. 3: Reconsidering the system given by (20), sag is modelled in phases a and b ., which can be considered LLG (double line to ground) fault and is treated as dual or double phase sag. This phenomenon can occur in any two phases. In this case of double sag, the magnitude is $V_{sag} = 0.1$,

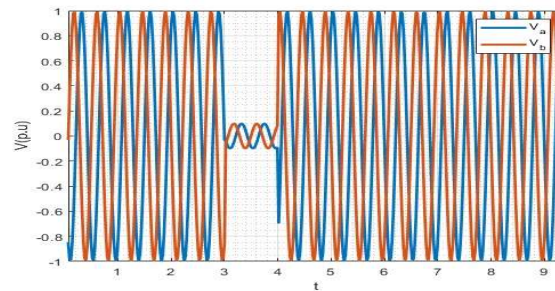


Figure 9 Double phase sag phase ab) IN 2d

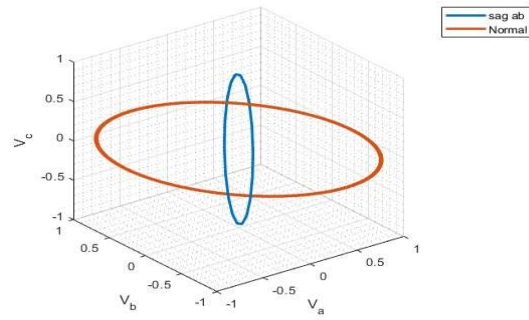


Figure 10 Double phase sag (phase ab)

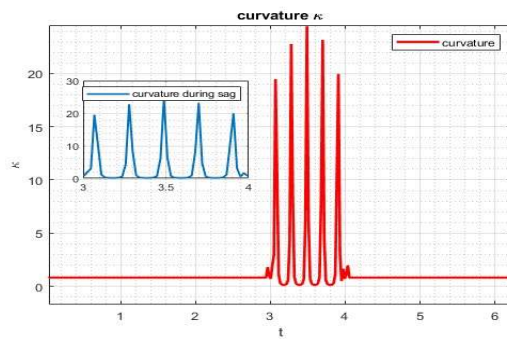


Figure 11 Curvature index

Fig. 9, 10, and 11, respectively, signify the double-phase sag and its representation in the *TNB* frame compared to the regular system (no sag) and the curvature index.

Case. 4: This case presents the sag in all three phases of the system represented by (16)-(18), which can be perceived as a particular case due to *LLL* (triple line) fault, and the sag value is 0.1 p.u.

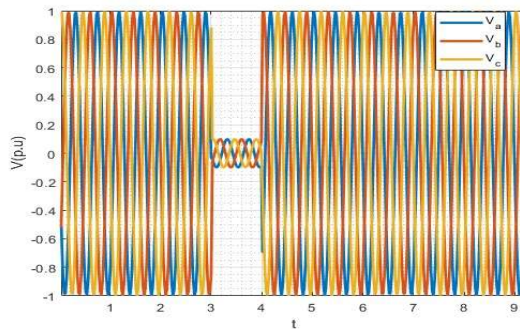


Figure 12 Triple phase sag

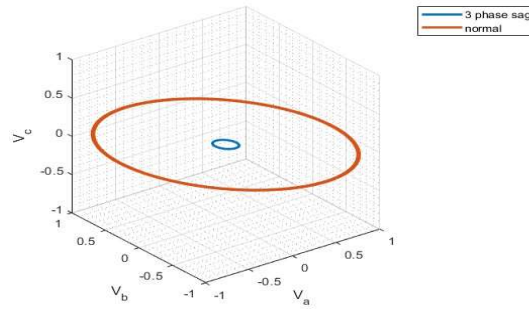


Figure 13. Triple phase sag in *TNB*

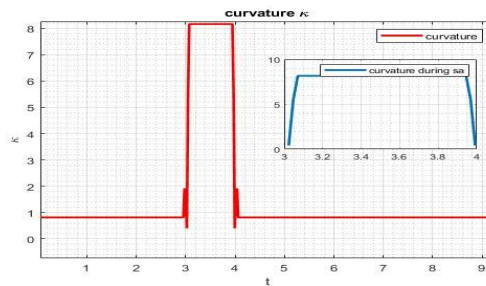


Figure 14 Curvature index for triple-phase sag

Figures 12 and 13 illustrate the three-phase sag and its representation in the TNB or Frenet frame. Figure 14 shows the suggested curvature index for the three-phase event. Consequently, all of the single sag occurrences, as well as the multistage sag event [3], maybe appropriately portrayed within the mathematical framework of differential geometry, as shown in Fig. 15. The abnormal occurrence and its trajectory may both be correctly explained using the three-dimensional visualisation of orthonormal vector.

Case. 5

The proposed mathematical approach has been validated by the raw EPRI data [23]. Although some earlier works have shown a mathematical approach using this data in Clark components, where the signals have been pre-processed for clarity of understanding, we would like to propose the approach without pre-processing of data. Table II presents the results for different events and their geometric representation.

In Fig 16. Three cases of the recorded waveform have been shown where (a) represents a single-phase sag event, (b) represents a three-phase sag event, (c) represents a double-phase sag event and (d) is a replica in the α - β plane for signal 3555 to show the ability of Frenet frame in successfully representing an α - β plane in TNB plane. The subsequent distortions in the trajectory of the ellipse are due to the presence of harmonics in signals, and the presence of torsion values well supports the fact that the Frenet frame's torsion value for a balanced and disturbance-free signal is 0.

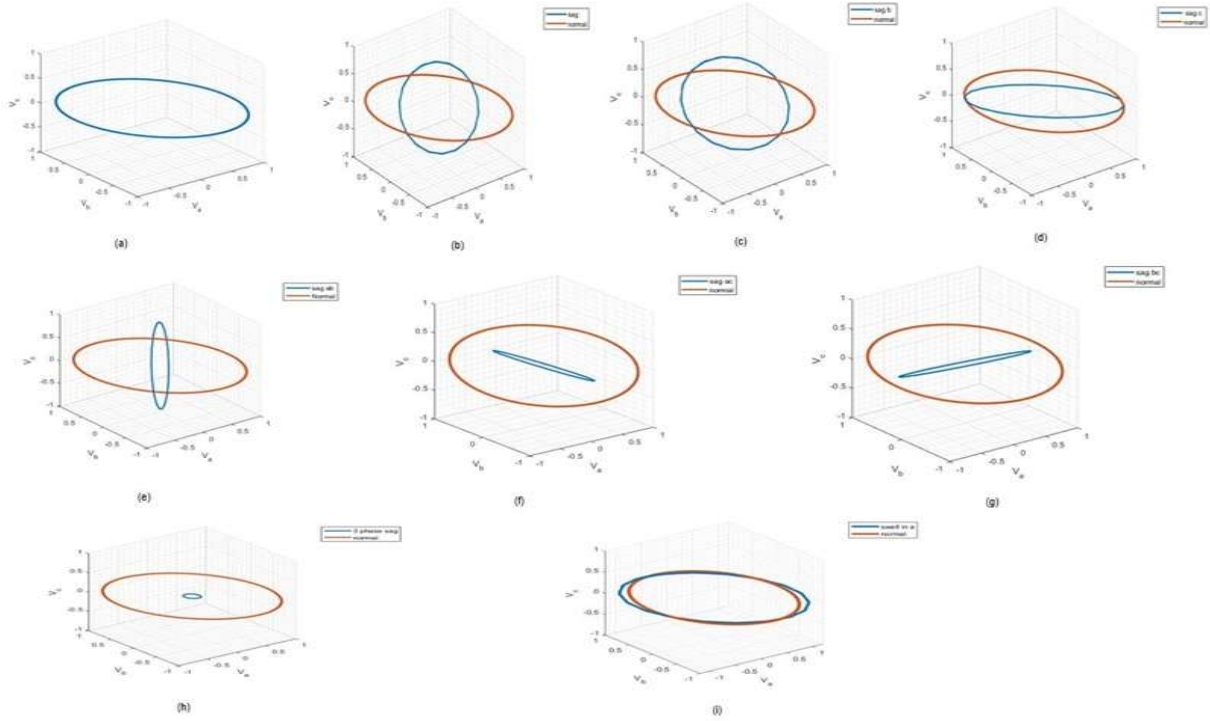
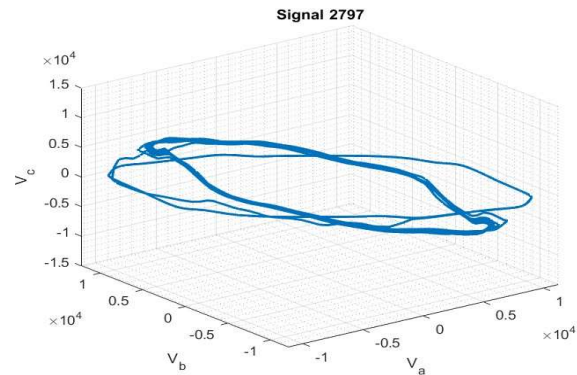


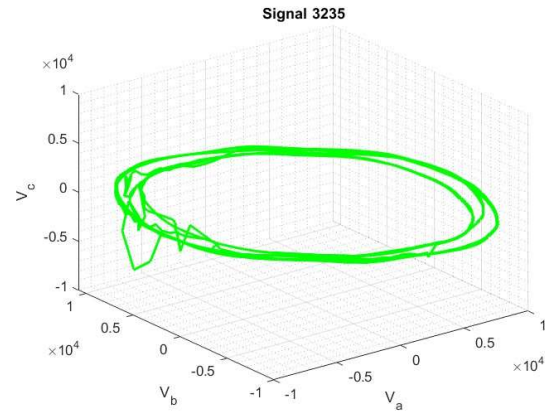
Figure 15 (a) represents a healthy system(no sag),(b)-(d) represents the sag in a,b, and c, individually, (e)-(g) represents double phase sag in the order ab, bc, and ac, (h) represents three phase sag and (i) represents a swell of 1.1 p.u. in phase a

Table II: curvature index for a sag of 0.1 p.u.

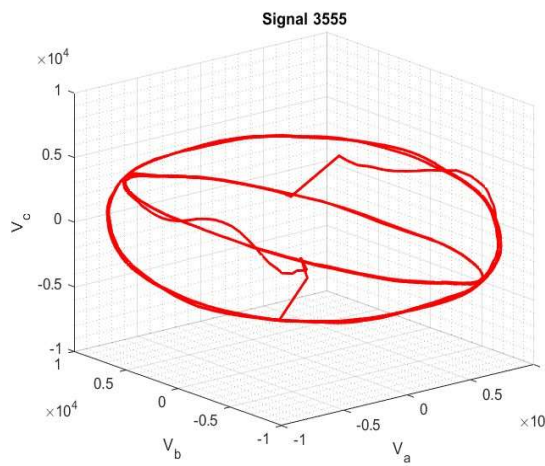
Signal No	Curvature index	Angle
2797	$3.16 \cdot 10^{-6} \leq k \leq 0.0042$	90°
2911	$7.3 \cdot 10^{-6} \leq k \leq 0.0015$	30°
2948	$3.5 \cdot 10^{-6} \leq k \leq 0.0132$	90°
2912	$1.93 \cdot 10^{-6} \leq k \leq 0.0018$	30°
3555	$1.4 \cdot 10^{-8} \leq k \leq 0.0022$	60°
3235	$0.00008 \leq k \leq 0.0053$	0°



(a)



(b)



(c)

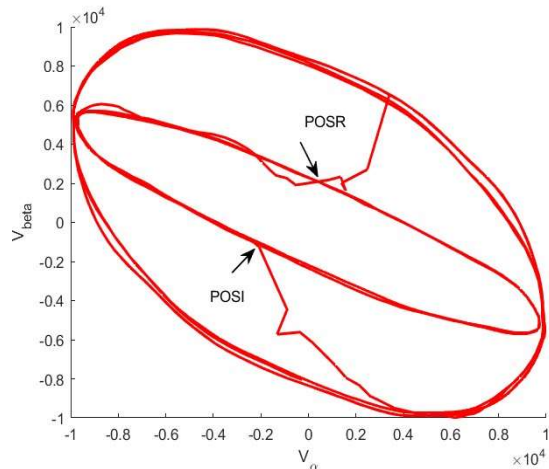


Figure 16 Voltage trajectory in TNB for (a) signal 2797 (b) signal 3235 (c) signal 3555 (d) voltage trajectory in α - β frame

5. Results and discussion

The case studies discussed in the previous section provide a thorough representation of the sag characteristics in a three-phase system. Additionally, the differential geometric framework concerned with the sag and swell

analysis offers a new interpretation of curvature. As a more general retrospection, particularly in the case of a single sag event, such as sag in phase a, when the depth(d) of sag varies from 0.1 p.u. to 0.9 p.u., some interesting phenomena are observed. Let us reproduce these scenarios in 2-D for a more accurate visual understanding in Fig.17 and 18.

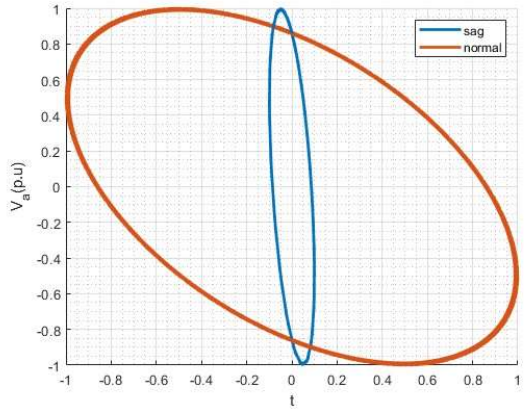


Figure 17 0.1 p.u. sag in phase a

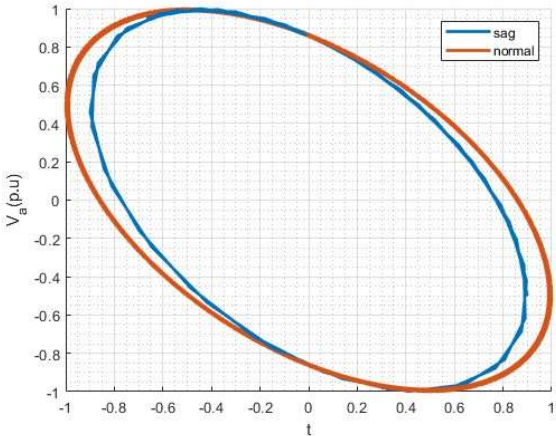


Figure 18 0.9 p.u. Sag in phase a

When the depth of sag is changed, the inclination also shifts, and so does the curvature. This can be inferred from Tables II and III, which provide a numeric representation of curvature values so that they can be understood as numeric values at various points along the voltage trajectory. This depiction makes it easy to comprehend that the inclination shifts when the sag's depth changes.

From Tables II and III, it can be understood how the change in the depth of sag gives the oscillating value of curvature and how it is related to the geometric indicator curvature (κ), as described in (21) and (22). The healthy state in Tables II and III refers to the system free of voltage variation or sag(dip). A dip is when a single or multiphase voltage variation(sag) event occurs. Also from Table I, the results and angle can be interpreted. However, there is a difference in the curvature range of simulated cases and recorded waveform,

primarily because simulated cases are just for mathematical understanding, and the disturbance attribution is random. However, still, the instances convey a general observation of sag and swell.

Table III: curvature index for a sag of 0.1 p.u.

Type of Sag	Curvature index(κ_{index}) (For a dip of 0.1 p.u.)
Single-phase Voltage Dip(sag) (Signature- B, D, F)	$0.1 \leq \kappa \leq 2.5$ (healthy state) $1 \leq \kappa \leq 2.5$ (dip)
Double-phase Voltage Dip (Signature- C, E, G)	$1 \leq \kappa \leq 16.5$ (healthy state) $3 \leq \kappa \leq 16.5$ (dip)
Three-phase Voltage Dip (Signature- A)	$1.5 \leq \kappa \leq 8$ (healthy state) $6.5 \leq \kappa \leq 8$ (dip)

Table IV: curvature index for a sag of 0.9 p.u.

Type of Sag	Curvature index(κ_{index}) (For a dip of 0.9 p.u.)
Single-phase Voltage sag (Signature- B, D, F)	$0.4098 \leq \kappa \leq 0.9798$ (healthy state) $0.7013 \leq \kappa \leq 0.9272$ (dip)
Double-phase Voltage Dip (Signature- C, E, G)	$0.4098 \leq \kappa \leq 1.0020$ (healthy state) $0.6218 \leq \kappa \leq 0.9643$ (dip)
Three-phase Voltage Dip (Signature- A)	$0.4098 \leq \kappa \leq 1.0185$ (healthy state) $0.6780 \leq \kappa \leq 0.9072$ (dip)

The sag angle, measured from the system's initial, healthy condition to the moment it sags, may be determined using (15). In this representation, a few exciting achievements may be highlighted, most notably:

- I. In the event of voltage variation in one of the phases, e.g., in phase a, the tilt angle is $\pi/2$. It is progressively scaled by a factor of 1/3 for subsequent events in phases b and c.
- II. The curvature numeric values for sag involving two phases are maximum Table.II and the tilt angle are in the multiple of $\pi/3$ for double phase sag ab ; later on, for phase ac, it is $2\pi/3$, and so on.
- III. The inclination angle is zero for a three-phase sag.

The inclination angle varies even if the sag depth varies for the same phase, Fig. 15 and 16. Finally, Fig. 19 shows a spatiotemporal 3-D picture of a typical three-phase system with 0.1 p.u. Sag and 1.1 p.u. Swell in phase 'a'.

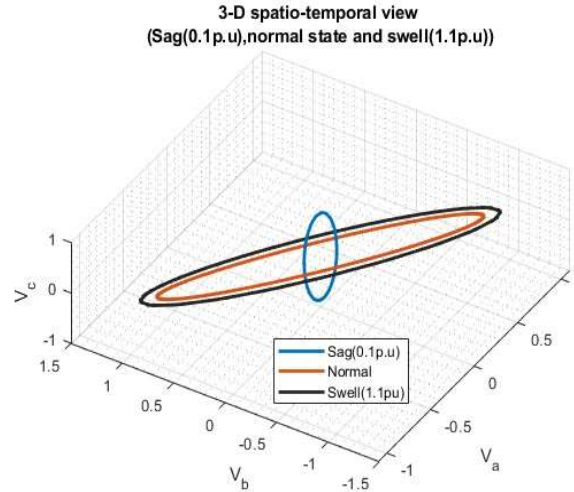


Figure 19 3-d differential view of voltage variation

6. Conclusion

This article proposes a new concept for the characterisation or pattern recognition of sag and swells based on a local vector property in differential geometry. The authors conceived the notion of this research. The sag-swell shape analysis is provided in three dimensions, providing a more accurate geometric viewpoint. The present study introduces a novel geometrical analytic approach for describing power system voltage sag and swell events. By employing differential geometry, particularly the concept of curvature, we gain a fresh perspective on understanding these power quality phenomena. The traditional methods, such as the Clark and Park transformation and RMS method, have been prevalent in sag characterisation, but they cannot capture detailed waveform shape information.

In contrast, the proposed curvature-based method allows for a more comprehensive analysis of voltage sag and swell events. The curvature profile obtained from the practical signal data reveals distinct patterns and variations in the voltage waveforms, providing deeper insights into the shape and behaviour of these events. This approach enhances our ability to distinguish between different types of sags, such as single-phase, double-phase, and three-phase sags, based on their curvature characteristics.

The geometric analysis here contrasts with the complex algebra-based space vector technique. These simulated case studies assume no noise or interference. The given study further improves knowledge of ellipse geometry utilised for power quality and how curvature might be connected to the major and minor axis.

Appendix

e_1, e_2, e_3 : Euclidean coordinate

T: Tangent vector

N: Normal vector

B: Binormal vector

GA: Geometrical Algebra

DG: Differential geometry

κ : curvature

τ : torsion

d: sag depth

θ : inclination angle

$\beta=120$; phase difference angle

POSI: point of sag initiation

POSR: point of sag retardation

G_3 : 3-D Euclidean geometric algebra

References

- [1] J. M. Aller, A. Bueno, and T. Paga, "Power system analysis using space-vector transformation," in IEEE Transactions on Power Systems, vol. 17, no. 4, pp. 957-965, Nov. 2002, DOI: 10.1109/TPWRS.2002.804995.
- [2] V. Ignatova, P. Granjon and S. Bacha, "Space Vector Method for Voltage Dips and Swells Analysis," in IEEE Transactions on Power Delivery, vol. 24, no. 4, pp. 2054-2061, Oct. 2009, DOI: 10.1109/TPWRD.2009.2028787.
- [3] M. R. Alam, K. M. Muttaqi and A. Bouzardoum, "Characterising Voltage Sags and Swells Using Three-Phase Voltage Ellipse Parameters," in IEEE Transactions on Industry Applications, vol. 51, no. 4, pp. 2780-2790, July-Aug. 2015, doi: 10.1109/TIA.2015.2397176.
- [4] J. Lira, V. Cardenas, and C. Nunez, "Factor compensation capacity," (ICEEE). 1st International Conference on Electrical and Electronics Engineering, 2004., 2004, pp. 567-572, DOI: 10.1109/ICEEE.2004.1433949.
- [5] M. R. Alam, K. M. Muttaqi and A. Bouzardoum, "A New Approach for Classification and Characterisation of Voltage Dips and Swells Using 3-D Polarization Ellipse Parameters," in IEEE Transactions on Power Delivery, vol. 30, no. 3, pp. 1344-1353, June 2015, DOI: 10.1109/TPWRD.2014.2361624.
- [6] M. Faisal, M. S. Alam, M. I. M. Arafat, M. M. Rahman, and S. M. G. Mostafa, "PI controller and park's transformation based control of dynamic voltage restorer for voltage sag minimisation," 2014 9th International Forum on Strategic Technology (IFOST), 2014, pp. 276-279, DOI: 10.1109/IFOST.2014.6991121.
- [7] Mostafa Bakkar, Santiago Bogarra, Alejandro Rolán, Felipe Córcoles, Jaume Saura, Voltage sag influence on controlled three-phase grid-connected inverters according to the Spanish grid code, IET Generation, Transmission & Distribution, 10.1049/iet-gtd.2019.1496, 14, 10, (1882-1892), (2020).
- [8] M. Paolone et al., "Fundamentals of power systems modeling in the presence of converter-interfaced generation," Electric Power Systems Research, Volume 189, 2020, 106811, ISSN 0378-7796, <https://doi.org/10.1016/j.epsr.2020.106811>.

- [9] F. Milano, "The Frenet Frame as a Generalization of the Park Transform," in *IEEE Transactions on Circuits and Systems I: Regular Papers*, vol. 70, no. 2, pp. 966-976, Feb. 2023, doi: 10.1109/TCSI.2022.3223726
- [10] "IEEE Recommended Practice for Monitoring Electric Power Quality," in *IEEE Std 1159-2019 (Revision of IEEE Std 1159-2009)*, vol., no., pp.1-98, 13 Aug. 2019, doi: 10.1109/IEEESTD.2019.8796486
- [11] D. Hestenes, G. Sobczyk, *Clifford Algebra to Geometric Calculus: A Unified Language for Mathematics and Physics*, Kluwer Academic, 1987.
- [12] E. Bayro-Corrochano. *Geometric Algebra Applications Vol.I: Computer Vision. Graphics and Neurocomputing*. Springer Verlag 2019.
- [13] M. P. do Carmo, *Differential Geometry of Curves and Surfaces*. Prentice-Hall, Inc Englewood Cliffs, New Jersey, 1976
- [14] E. J. Bayro-Corrochano, G. Altamirano-Escobedo, A. Ortiz-Gonzalez, V. Farias-Moreno, and N. Chel-Puc, "Computing in the Conformal Space Objects, Incidence Relations, and Geometric Constrains for Applications in AI, GIS, Graphics, Robotics, and Human-Machine Interaction," in *IEEE Access*, vol. 10, pp. 112742-112756, 2022, doi: 10.1109/ACCESS.2022.3216266.
- [15] SZ. Djokic, J.V. Milanovic, D.J. Chapman, and M.F. McGranaghan, "Shortfalls of existing methods for classification and presentation of voltage reduction events", *IEEE Trans. on Power Delivery*, vol.20, no.2, pp. 1640–1649, Apr. 2005.
- [16] S. Stramigioli, A. van der Schaft, B. Maschke and C. Melchiorri, "Geometric scattering in robotic telemanipulation," in *IEEE Transactions on Robotics and Automation*, vol. 18, no. 4, pp. 588-596, Aug. 2002, DOI: 10.1109/TRA.2002.802200.
- [17] H. Hajieghrary, D. Kularatne, and M. A. Hsieh, "Differential Geometric Approach to Trajectory Planning: Cooperative Transport by a Team of Autonomous Marine Vehicles," 2018 Annual American Control Conference (ACC), 2018, pp. 858-863, DOI: 10.23919/ACC.2018.8430951.
- [18] F. Milano, "A Geometrical Interpretation of Frequency," in *IEEE Transactions on Power Systems*, vol. 37, no. 1, pp. 816-819, Jan. 2022, DOI: 10.1109/TPWRS.2021.3108915.
- [19] F. Milano, G. Tzounas, I. Dassios, and T. Kërçi, "Applications of the Frenet Frame to Electric Circuits," in *IEEE Transactions on Circuits and Systems I: Regular Papers*, vol. 69, no. 4, pp. 1668-1680, April 2022, DOI: 10.1109/TCSI.2021.3133948.
- [20] J. R. Camarillo-Peñaranda and G. Ramos, "Characterisation of Voltage Sags Due to Faults in Radial Systems Using Three-Phase Voltage Ellipse Parameters," in *IEEE Transactions on Industry Applications*, vol. 54, no. 3, pp. 2032-2040, May-June 2018, doi: 10.1109/TIA.2018.2793245.
- [21] J. R. Camarillo-Peñaranda and G. Ramos, "Fault Classification and Voltage Sag Parameter Computation Using Voltage Ellipses," in *IEEE Transactions on Industry Applications*, vol. 55, no. 1, pp. 92-97, Jan.-Feb. 2019, doi: 10.1109/TIA.2018.2864108.
- [22] M. R. Alam, F. Bai, R. Yan and T. K. Saha, "Classification and Visualisation of Power Quality Disturbance-Events Using Space Vector Ellipse in Complex Plane," in *IEEE Transactions on Power Delivery*, vol. 36, no. 3, pp. 1380-1389, June 2021, doi: 10.1109/TPWRD.2020.3008003.

[23] "DOE Disturbance Library," US Dept. Energy Electr. Power Res. Inst., Orlando, FL, USA. [Online]. Available: http://pqmon.epri.com/disturbance_library/see_all.asp